2012 NDIA GROUND VEHICLE SYSTEMS ENGINEERING AND TECHNOLOGY SYMPOSIUM
MODELING & SIMULATION, TESTING AND VALIDATION (MSTV) MINI-SYMPOSIUM
AUGUST 14-16, MICHIGAN

DEVELOPMENT OF LABORATORY TESTING APPARATUS AND FATIGUE ANALYSIS FOR TRACKED VEHICLE RUBBER BACKER PADS

Daniel Kujawski, Ph.D.
Department of Mechanical and Aeronautical Engineering
Western Michigan University
Kalamazoo, MI 49008-5343

Daren DiStefano
Department of Mechanical and Aeronautical Engineering
Western Michigan University
Kalamazoo, MI 49008-5343

William Bradford
US Army RDE Command (RDECOM)
Track and Suspension Group, Warren, MI 48397-5000

ABSTRACT

The first part of this paper will outline the conception of the testing apparatus (Figure 1), along with its operation and preliminary results. The second part of the paper will discuss a new methodology used to correlate the dependence of crack growth rate for strain crystallizing natural rubbers in terms of tearing energy. The tearing energy which depends on the type of elastomer, geometry and stress strain behavior of a particular specimen demonstrates a direct correlation with the crack growth rate at different R-ratios (= min tearing energy/max tearing energy).

INTRODUCTION

Track components for military tanks provide essential traction and support for propulsion and maneuvering of the vehicle. Due to the extremely high stresses in extension, compression, and shear, which these components experience during the normal operation of tracked vehicles, the elastomeric components become the life limiter of the track system. Increases in vehicle weight, severe operating environments, and requirements for higher operability has significantly challenged the durability and reliability of the track system and components. Improving the durability, reliability of track components and systems has a significant impact on life cycle costs, logistics, field support, and vehicle/war fighter effectiveness.

The Elastomer Improvement Program (EIP) within TARDEC's Ground Vehicle Power Mobility (GVPM) group has invested in an R&D laboratory which specializes in high temperature testing to characterize failure mechanisms of track components and identify key property sets that will drive durability improvements. This capability has been leveraged to identify the various failure modes of track bushings, ground pads, road wheel backer pads (RWBP), and road wheels. EIP activities are driven by a 3 Phase process: 1) Identify and understand failure modes; 2A) Leverage finite element analysis (FEA); 2B) Develop customized tests components that mimic failure modes, screen improvements; 2C) Optimize durability through material and design; 3A) Validation on vehicle platforms; 3B) Modify requirements and specifications.

The Phase 3 activities are time consuming and very expensive considering vehicle tests can cost from $0.5 M - $1.0 M per test. Consequently R&D activities can be accelerated by adopting customized component test, which provide R&D direction on down selecting material and design improvements. The EIP lab has developed customized tests for the track bushing and road wheel, the ground pad and road wheel backer pad tests are in development.

The Fatigue and Fracture Lab at Western Michigan University (WMU) has partnered with TARDEC's EIP lab to develop a customized test for an Abrams T-158LL RWBP. The first part of this paper will outline the conception of the testing apparatus along with its operation and preliminary results.

The second part of the paper will discuss a new methodology used to correlate the dependence of crack

growth rate for strain crystallizing natural rubbers in terms of tearing energy. The tearing energy, which depends on the type of specimen's geometry and stress strain behavior of a particular elastomer, demonstrates a direct correlation with the crack growth rate at different tearing energy ratios, R (= min tearing energy/max tearing energy). In the case of filled styrene-butadiene rubbers, a single curve can represent this relationship for any R-ratio applied to a given specimen. However, in the case of filled natural rubbers the phenomenon of strain crystallization causes shifts in the tearing energy curves dependent on the applied R-ratio. For this reason, a new methodology is proposed that has a high potential to predict the fatigue life using the tearing energy curves and the R-ratios applied.

TESTING APPARATUS

An apparatus has been designed that can allow for testing of backer pads in a laboratory setting. There are numerous advantages to testing in this way. Laboratory testing requires substantially less funding, and by changing the severity of the testing conditions time to failure for the rubber pad can be increased or decreased. Additionally, the environmentally controlled laboratory setting allows for the use of instrumentation to gather detailed data such as load history, temperature, hardness, etc…

However, the task of replicating the amount of damage sustained by a rubber pad during the operation of a vehicle, such as the 60 ton Abram tank, in a laboratory setting is plagued with challenges. Elastomers are extremely sensitive to loading conditions and geometry. For this reason, it is difficult to duplicate the actual service damage by testing a sample of the material. The full-scale testing preserves the pad's geometry and potentially may duplicate the actual field damage. Essentially, in order to have an accurate test a rubber pad needs to be passed under a road wheel that is exerting the force that would be realized in the field, at a speed comparable to the operating speed of the vehicle.

The estimated force exerted between the road wheel and the backer pad is in the ranges of 3,000 to 10,000 lbs. This requires a powerful machine with substantial size. For this reason, an MTS biaxial universal testing machine was selected as the base of the testing apparatus. The machine is capable of withstanding all the forces necessary to accurately simulate the loads that are experienced by the backer pad in even the largest armored vehicle. It is capable of applying up to 100,000 lbs of compressive load. Additionally, the machine is large enough to accommodate the modifications necessary to impart linear motion on the backer pad, Figure 1.

The next challenge was designing a way to impart linear motion to the full-scale tank pad under the desired load. After numerous designs, an efficient and robust design was settled upon. A carriage houses the backer pad and is affixed to two double ainsi 60 chains that are driven by a 10 hp motor which is controlled by a 60 Hz frequency inverter controller. The system is capable of driving the carriage at speeds up to 35 mph with a resolution of 0.006 mph. In addition, a tank wheel is affixed to the load cell of the MTS machine accurately simulating the distributed loads the rubber would experience in the field.

Once the method for driving the rubber backer pad was determined, the next challenge was designing a suspension system for the carriage housing the buggy that would quietly and safely transport the assembly across the testing apparatus. In order to accomplish this, six Hevi-Rail HVB-053 bearings were selected, each of which is capable of withstanding 5,400 lbs of dynamic load in the radial direction, and 2,250 lbs of dynamic load in the axial direction. Additionally, the spatial dimensions are within the geometric constraints imposed by the dimensions of the buggy and the clearance heights of the testing apparatus.

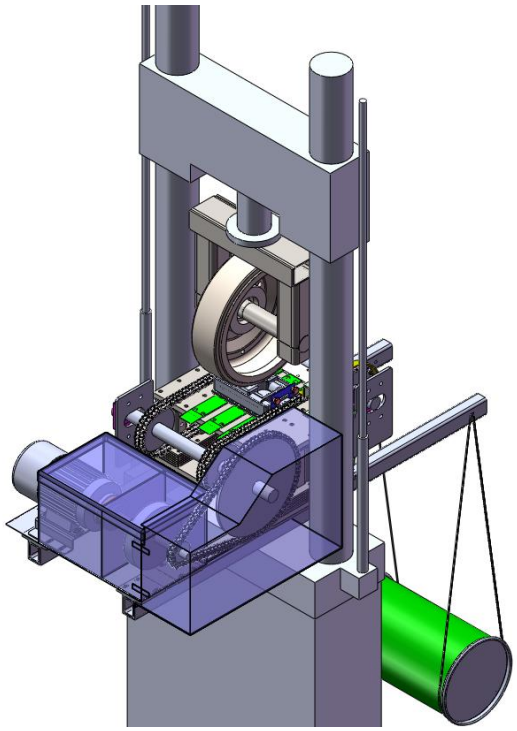

Figure 1: Schematic of the testing apparatus

The resulting test apparatus is capable of accurately replicating the complex loading conditions that would be experienced during real world use. The combination of accurately simulated loading conditions, with laboratory instrumentation allows for a wealth of information to be gathered. For example, when examining the loading history, it can be observed that the peak load increases after the first

minutes of testing, due to the hardening of the rubber, Figure 2a. Through the entire time of the test the peak load experienced by the rubber backer pad varies about +/- 500 lbs, Figure 2b. Additionally, upon closer inspection of the loading history it can be observed that the peak load decreases when the wheel is directly at the middle of the rubber backer pad, Figure 2c. These observations need to be considered when deriving a model for the loading, and could not be observed outside of a laboratory setting.

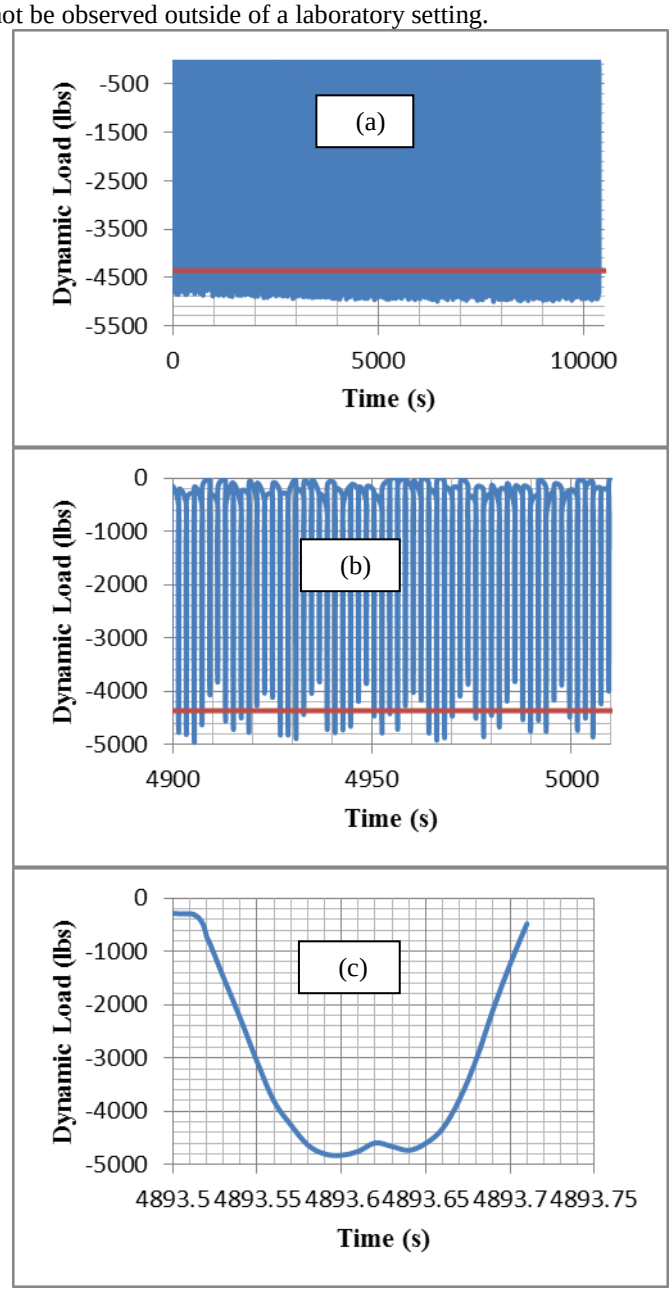

Figure 2: Loading history of rubber backer pad with respect to time for different time intervals; (a) 10,000 s, (b) 100 s, and (c) one loading cycle.

Currently, future work is being focused on incorporating other factors experienced by the rubber in real world use, such as elevated temperature and abrasion.

Tearing Energy

Tearing energy is the most widely used loading parameter when considering fatigue in elastomers. The tearing energy depends on specimen's geometry and the stress strain behavior of a particular rubber. Most importantly, there is a direct correlation between the fatigue crack growth rate, da/dN, and tearing energy, T.

In general, the relationship between the crack growth rate and tearing energy is that of a power-law.

$$\frac{da}{dN} = C \cdot (T)^m \qquad (1)$$

In Eq. (1) C and m are constants used for fitting the data. Usually, for filled styrene-butadiene rubbers (SBR) a specimen can be fit with the same constants for all R-ratios. However, in the case of filled natural rubber (NR) the occurrence of strain crystallization results in significantly different curves for different R-ratios.

When examining the crack growth curves of elastomers in Figure 3, there are four distinct regions noted (Lake and Lindley, 1965).

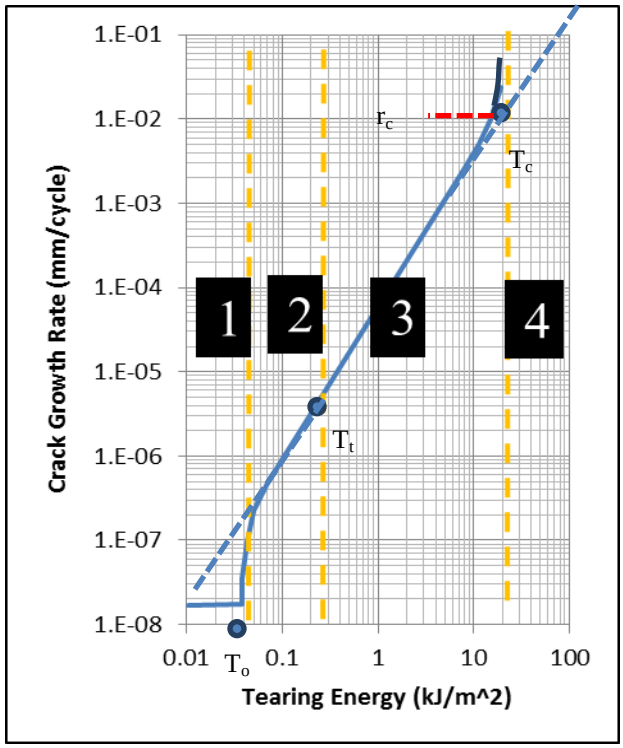

Figure 3: Tearing energy vs. crack growth rate curve

In the first region in Figure 3, the tearing energy is below the tearing energy required to cause crack growth. This tearing energy will be referred to as the threshold tearing energy, T_0. Once the tearing energy exceeds the threshold, the crack growth rate follows a linear relationship up to the transition tearing energy, T_t. The crack growth rate at region 2 can be fitted by the following equation.

$$\frac{da}{dN} = A \cdot \left| T - T_o \right| \tag{2}$$

where A is a constant used to fit the data (Mars and Fatemi, 2003).

The 3rd region spans from T_t to a critical tearing energy, T_c, above which, crack growth becomes unstable. This is the region that follows the power law relationship.

The fourth region encompasses T greater than T_c until failure.

Traditional Approach for Correlating R-ratio Effects

The first assumption made is that regions 1, 2, and 4 depicted in Figure 3 are negligible and therefore, the entire curve can be approximated with a power law relationship, as within the 3rd region.

When observing multiple R-ratio curves, da/dN vs. T, for a given specimen it is clear that all curves share a common point right before crack growth becomes unstable, Figure 4.

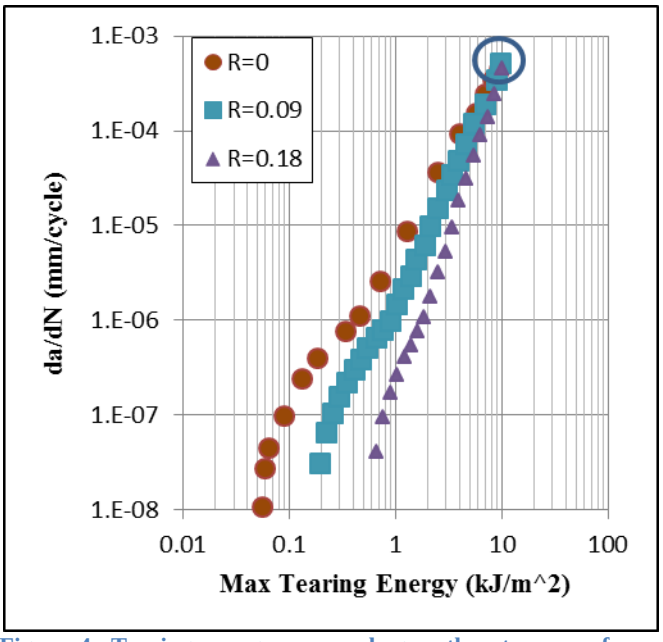

Figure 4: Tearing energy vs. crack growth rate curve for three different R-ratios (Mars, 2009).

This common point denotes a critical crack growth rate, r_c, and corresponding critical tearing energy, T_c, for a material regardless of the R-ratio. Mars and Fatemi (2003) realized the significance of these values as material properties, and incorporated them into their model, given by Eq. (3).

$$\frac{da}{dN} = r_c \cdot \left(\frac{T}{T_c} \right)^F \tag{3}$$

where T_c and r_c are the critical tearing energy and crack growth rate, respectively and F is a constant used to fit the data determined from the 3rd region between T_t and T_c. Fitting of that model is shown in Figure 5.

Mars (2009) also realized that the slope F of the curve is directly related to the R-ratio being applied, Figure 6.

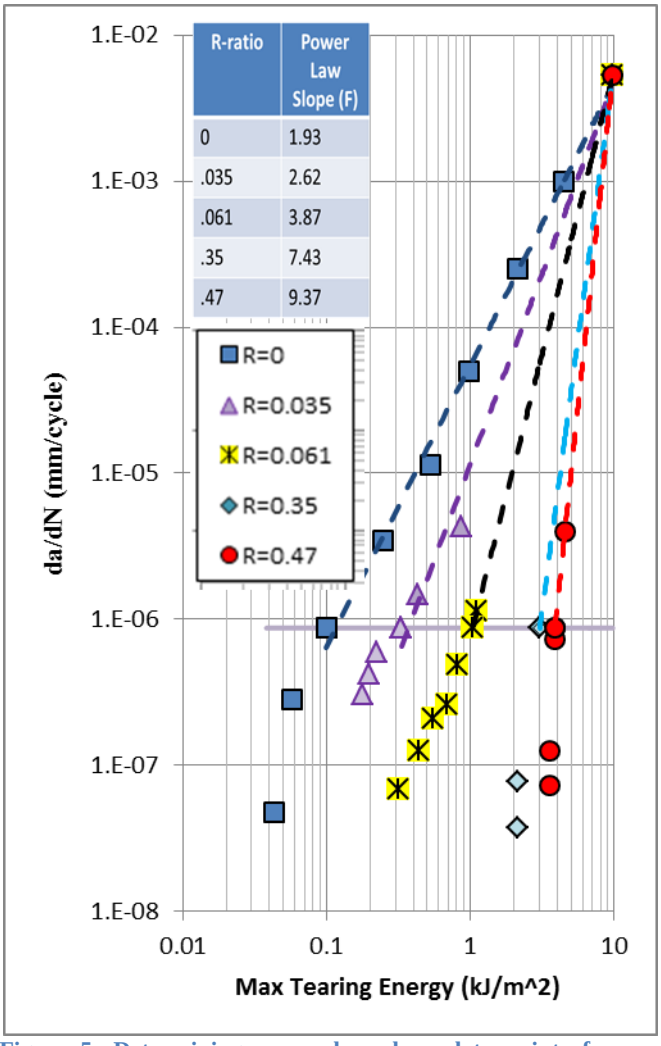

Figure 5: Determining power law slope data points from (Lindley, 1973)

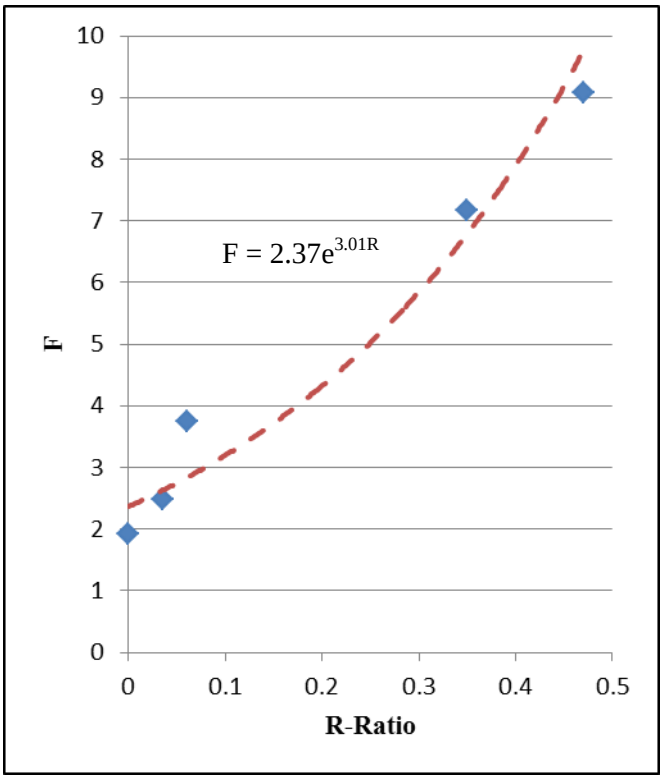

Figure 6: Slope dependence on R-ratio (from Fig.5).

In this study, the relationship between the slope F and the R-ratio have been fitted using an exponential relationship, Figure 6. Others have suggested, that the data could be fitted using a polynomial relationship however, given the narrow range of R-ratios that have been examined, it is unlikely that a polynomial equation would successfully predict F values outside of that range.

Knowing the relationship between the slope F and the R-ratio allows for the curves of R-ratios other than zero to be plotted.

Mars and Fatemi (2003) proposed the use of an equivalent tearing energy T_{eq}. Considering two R-ratio curves one of which is R=0, T_{eq} would be the tearing energy that results in the same crack growth rate as the R=0 curve. T_{eq} can be calculated by setting da/dN for these two R-ratios equal to each other, Eq. (4) (Mars, 2009).

$$r_c \cdot \left(\frac{T}{T_c}\right)^{F_R} = r_c \cdot \left(\frac{T_{eq}}{T_c}\right)^{F} \tag{4}$$

Solving for T_{eq} and simplifying yields the following equation (5):

$$T_{eq} = T^{\frac{F_R}{F}} \cdot T_c^{\left(1-\frac{F_R}{F}\right)} \tag{5}$$

where F_R is the slope for that particular R-ratio.

This model has significant implications. By knowing the material properties T_c and r_c along with the relationship between the slope F and the R-ratio, the crack growth behavior can be predicted for any R-ratio, without needing to perform experimental testing.

This model can be used in one of two ways. The first of which is predicting the curve for a particular R-ratio. The first step of this process is selecting a range of tearing energies for which da/dN need to be predicted. For any tearing energy, T, the da/dN is calculated using Eq. (6). In Eq. 6), F_R corresponds to a particular R-ratio for which da/dN is calculated.

$$\frac{da}{dN} = r_c \cdot \left(\frac{T}{T_c}\right)^{F_R} \tag{6}$$

Finally, plotting Eq. (6) in terms of the tearing energy versus the calculated crack growth rates the predicted crack growth rate curves are obtained, Figure 7.

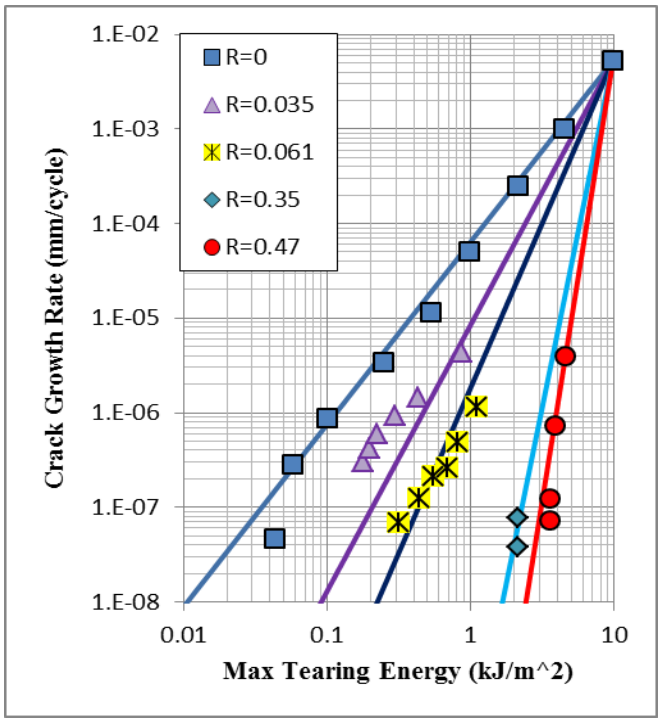

Figure 7: Traditional method: experiments vs. fitting.

This model can also be used to collapse all data points on to the R=0 curve. In order to accomplish this, the recorded experimental tearing energies are converted into their corresponding T_{eq} values and are then plotted against their experimental crack growth rates, Figure 8.

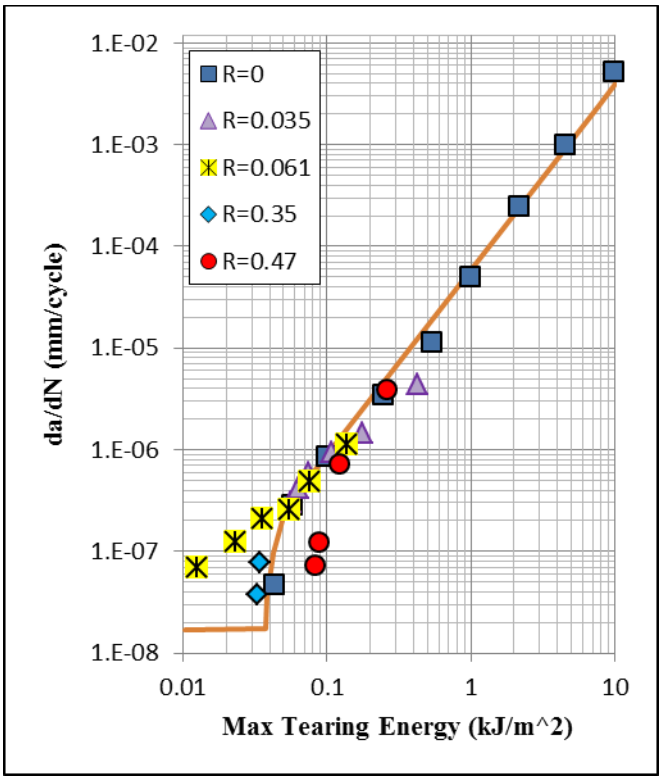

Figure 8: Traditional method for collapsing data

This method is particular beneficial because one can pick any crack growth rate of interest along the curve and use the following equation to determine the actual tearing energy, T, corresponding to the R-ratio of interest according to Eq. (7).

$$T = T_{eq}^{\frac{F}{F_R}} \cdot T_c^{\left(1-\frac{F}{F_R}\right)} \tag{7}$$

As a measure of the accuracy of this model, the experimental crack growth rates are plotted against the predicted rates, Figure 9. A perfect correlation would result in a 45° angle relationship.

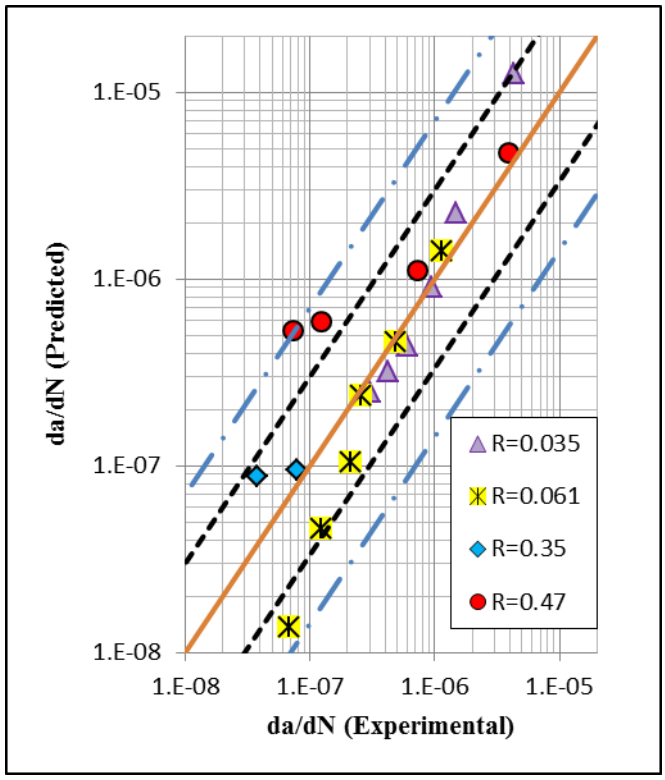

Figure 9: Error on life prediction from traditional model

From Figure 9 one can see that 100% of the predicted values are within seven times their corresponding experimental values, and 75% of the predicted values are within three times their corresponding experimental values. It should be noted, that although these errors seem rather drastic, when considering fatigue life predictions, an error within an order of magnitude is usually tolerable.

Modified Approach for Correlating R-ratio Effects

The traditional approach is an effective means of predicting fatigue crack growth data, and is relatively simple to use but it can lead to substantial error.

The largest amount of error from the traditional method occurs in the linear region of the curve, Figure 8. This is due to the assumption that this region is negligible. A model that includes this region will lead to a more accurate prediction of data.

The following method is based upon the previous method with the inclusion of the linear region. The first assumption for this model is that there is a common transition crack growth rate, r_t, which separates the linear and power law regions for all R-ratios. This transition crack growth rate is denoted by the dashed line in Figure 10.

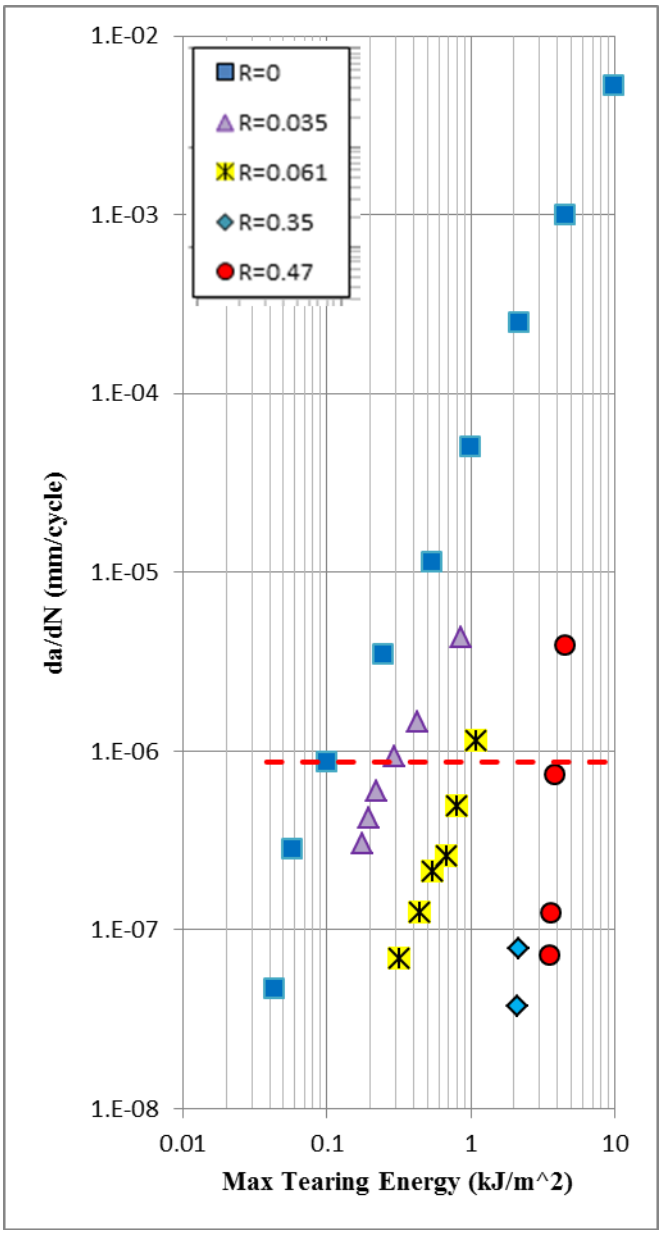

Figure 10: Separation of the main two regions

As with the previous method, the data points above the dashed line will be fitted using a power law relationship in order to determine F as a function of R-ratio. In addition to this, a linear relationship will be used to determine the threshold tearing energy, T_0, for each R-ratio curve. It was observed that these values are dependent upon the R-ratio in much the same way F is, Figure 11.

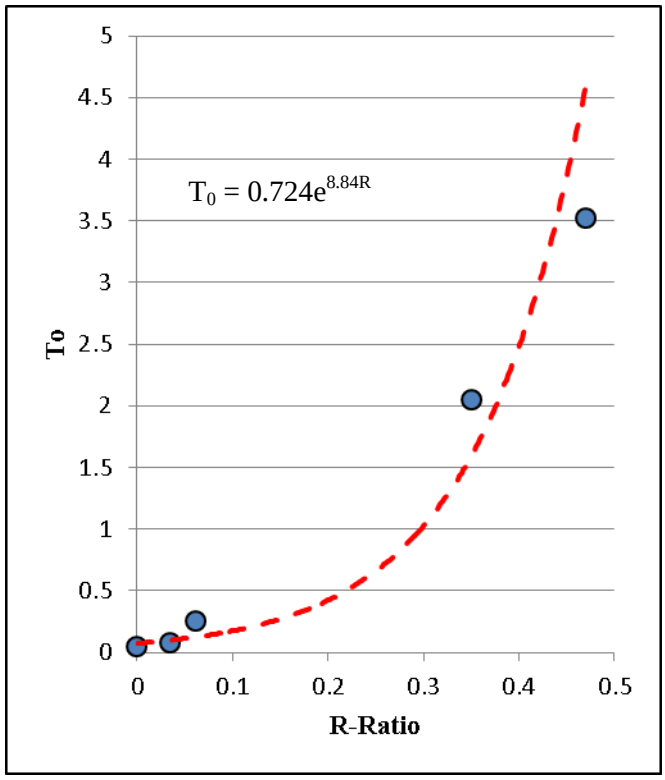

Figure 11: Dependence of T_o versus R-ratio

The proposed model incorporates the threshold tearing energy in order to more accurately predict the linear region. The theory behind this model stems from the large difference between T_o and the values of the tearing energy above T_t. In the linear region, the values of T and T_o are relatively similar and the difference between these two values is significantly lower than the corresponding tearing energy. However, above T_t the difference between T and T_o is nearly the same as the corresponding tearing energy. The modified model is described by Eq. (8).

$$\frac{da}{dN} = r_c \cdot \left(\frac{T_{eq}^{\ F} - T_o^{\ F}}{T_c^{\ F}} \right) \tag{8}$$

The methods for determining the slope F and T_o have been outlined in the previous section. Once they are determined, a single T_{eq} can be calculated according to Eq. (9) that will be used for both regions.

$$T_{eq} = \left(\frac{F_R}{T^{F}} - T_{oR}^{\frac{F_R}{F}} \right) \cdot T_C^{1-\frac{F_R}{F}} + T_o \qquad (9)$$

Equations (8) and (9) can be used to produce predicted curves depicted in Figure 12 or collapsed curves shown in Figure 13 for any R-ratio. The process for producing these curves is the same as with the traditional method outlined earlier.

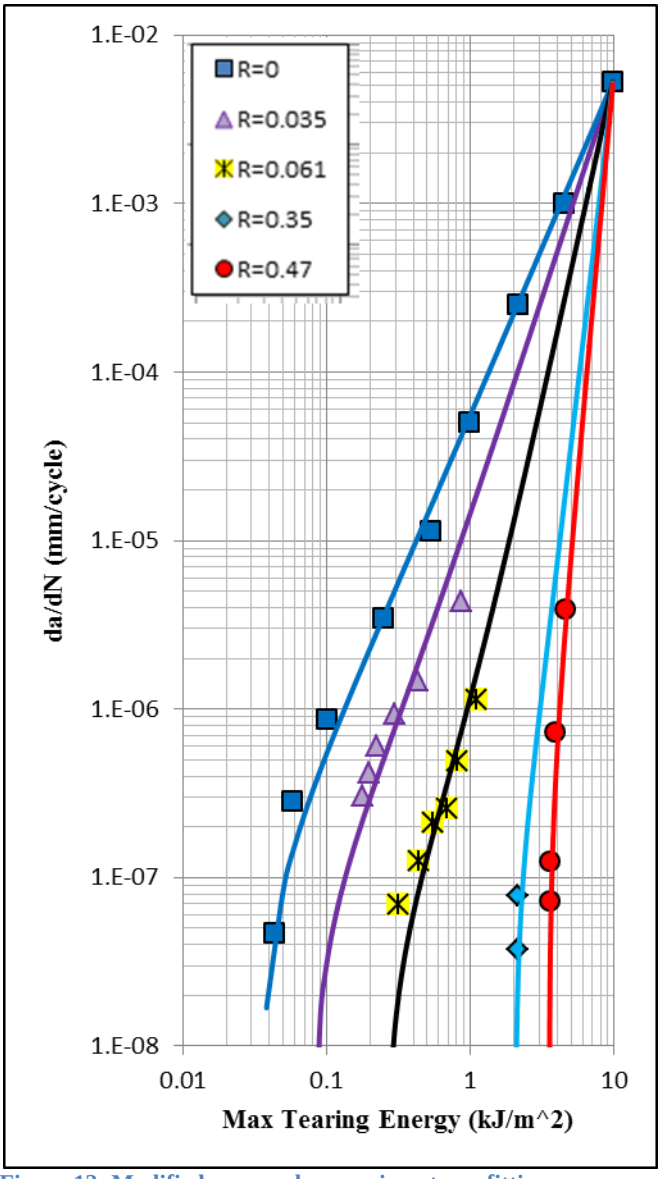

Figure 12: Modified approach: experiments vs. fitting.

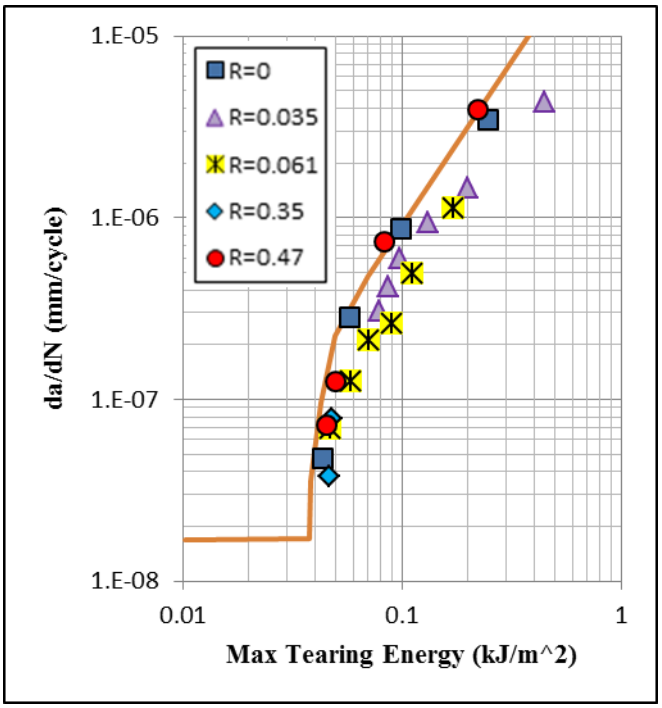

Figure 13: Modified approach collapsed data

Once again, the experimental crack growth rates will be compared with the predicted in order to quantify the accuracy of the model, Figure 14.

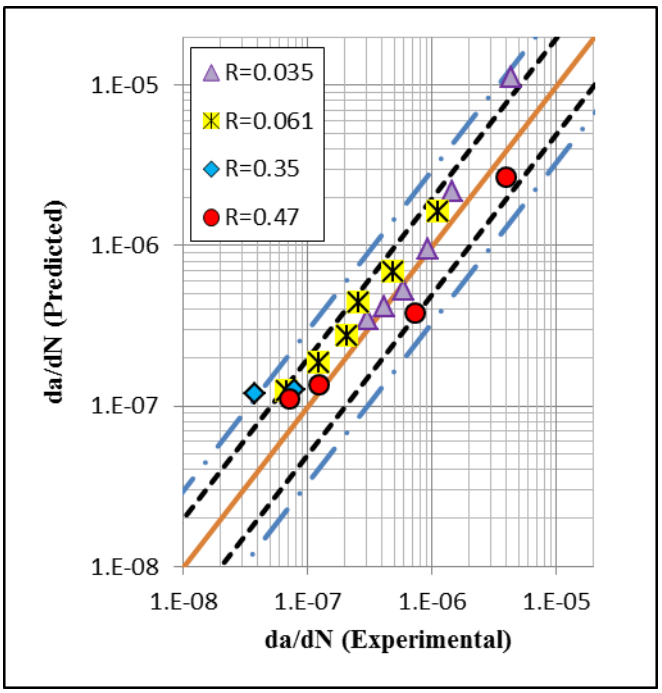

Figure 14: Modified approach life prediction

From Figure 14 one can see that 100% of the predicted values are within 3 times their corresponding experimental values, and 90% of the predicted values are within 2 times their corresponding experimental values.

This model allows for more accurate predictions of tearing energy versus crack growth rate relationship, especially for low crack-growth rates where parts spend most of their lives.

CONCLUSION

Significant efforts have been made by the military in order to develop an efficient way to screen different rubber compounds used for track backer pads. The methods outlined in this paper represent two potential avenues for accomplishing this goal. A testing apparatus has been developed, which is able to test newly developed components in a fraction of the time and cost field testing would require. Additionally, a new model was proposed for modeling and/or predicting the crack growth rate vs. tearing energy, which includes a slow-crack growth near the threshold region. This model provides a means for effective comparing/screening of fatigue properties of different rubber formulas.

ACKNOWLDGEMENTS

This investigation is supported by the MSU sub award No. 060803 360353. The Center for Advanced Vehicle Design and Simulation (CAViDS) and Fatigue and Fracture Laboratory at Western Michigan University has partnered with TARDEC's Elastomer Improvement Program (EIP) lab in this research.

REFERENCES

Lake, G., and Lindley, P. (1965). The Mechanical Fatigue Limit for Rubber. *Journal of Applied Polymer Science*, 348-364.

Lindley, P. (1973). Relation between hysteresis and the dynamic crack growth resistance of natural rubber. *International Journal of Fracture Vol. 9*, 449-461.

Mars, W. (2009). Computed Dependence of Rubber's Fatigue Behavior on Strain Crystallization. *Rubber Chemistry and Technology*, 51-61.

Mars, W., and Fatemi, A. (2003). A Phenomenological Model for the Effect f R ratio on Fatigue in Strain Crystallizing Rubbers. *Rubber Chemistry and Technology, Vol. 76, No 5*, 1241-1258.